J|A|C|S
ARTICLES
Published on Web 02/23/2007

Competing Electron-Transfer Pathways in Hydrocarbon Frameworks: Short-Circuiting Through-Bond Coupling by Nonbonded Contacts in Rigid U-Shaped Norbornylogous Systems Containing a Cavity-Bound Aromatic Pendant Group

Subhasis Chakrabarti,[†] Min Liu,[†] David H. Waldeck,*[,†] Anna M. Oliver,[‡] and Michael N. Paddon-Row*[,‡]

Contribution from the Chemistry Department, University of Pittsburgh, Pittsburgh, Pennsylvania 15260, and School of Chemistry, University of New South Wales, Sydney, New South Wales 2052, Australia

Received October 17, 2006; E-mail: dave@pitt.edu; m.paddonrow@unsw.edu.au

Abstract: This work explores electron transfer through nonbonded contacts in two U-shaped DBA molecules **1DBA** and **2DBA** by measuring electron-transfer rates in organic solvents of different polarities. These molecules have identical U-shaped norbornylogous frameworks, 12 bonds in length and with diphenyldimethoxynaphthalene (**DPMN**) donor and dicyanovinyl (**DCV**) acceptor groups fused at the ends. The U-shaped cavity of each molecule contains an aromatic pendant group of different electronic character, namely *p*-ethylphenyl, in **1DBA**, and *p*-methoxyphenyl, in **2DBA**. Electronic coupling matrix elements, Gibbs free energy, and reorganization energy were calculated from experimental photophysical data for these compounds, and the experimental results were compared with computational values. The magnitude of the electronic coupling for photoinduced charge separation, $|V_{CS}|$, in **1DBA** and **2DBA** were found to be 147 and 274 cm^{-1}, respectively, and suggests that the origin of this difference lies in the electronic nature of the pendant aromatic group and charge separation occurs by tunneling through the pendant group, rather than through the bridge. **2DBA**, but not **1DBA**, displayed charge transfer (CT) fluorescence in nonpolar and weakly polar solvents, and this observation enabled the electronic coupling for charge recombination, $|V_{CR}|$, in **2DBA** to be made, the magnitude of which is $\sim$ 500 cm^{-1}, significantly larger than that for charge separation. This difference is explained by changes in the geometry of the molecule in the relevant states; because of electrostatic effects, the donor and acceptor chromophores are about 1 Å closer to the pendant group in the charge-separated state than in the locally excited state. Consequently the through-pendant-group electronic coupling is stronger in the charge-separated state—which controls the CT fluorescence process—than in the locally excited state—which controls the charge separation process. The magnitude of $|V_{CR}|$ for **2DBA** is almost 2 orders of magnitude greater than that in **DMN-12-DCV**, having the same length bridge as for the former molecule, but lacking a pendant group. This result unequivocally demonstrates the operation of the through-pendant-group mechanism of electron transfer in the pendant-containing U-shaped systems of the type **1DBA** and **2DBA**.

Introduction

Electron-transfer reactions are a fundamental reaction type and are of intrinsic importance in biology, chemistry, and the emerging field of nanoscience.[1] Donor−bridge−acceptor (DBA) molecules allow systematic manipulation of the molecular properties[2−4] and provide an avenue to address important fundamental issues in electron transfer. For example, the U-shaped DBA molecules (in Scheme 1) hold the donor and the acceptor units at a fixed distance and conformation by a rigid hydrocarbon bridge and allow one to study the electron tunneling over a 5−10 Å distance scale. Placement of a pendant group in the cleft changes the electronic coupling magnitude between the donor and acceptor, thereby changing the electron-transfer rate. Previous work has shown that using an aromatic group as a pendant unit increases the electronic coupling, as compared to an aliphatic pendant,[5] but that different alkyl-

[†] University of Pittsburgh.
[‡] University of New South Wales.

(1) (a) Barbara, P. F.; Meyer, T. J.; Ratner, M. A. *J. Phys. Chem.* **1996**, *100*, 13148. (b) Jortner, J., Bixon, M., Eds. Electron Transfer-From Isolated Molecules to Biomolecules. In *Advances in Chemical Physics*; Wiley: New York, 1999.
(2) (a) Hush, N. S.; Paddon-Row, M. N.; Cotsaris, E.; Oevering, H.; Verhoeven, J. W.; Heppener, M. *Chem. Phys. Lett.* **1985**, *117*, 8. (b) Oliver, A. M.; Craig, D. C.; Paddon-Row, M. N.; Kroon, J.; Verhoeven, J. W. *Chem. Phys. Lett.* **1988**, *150*, 366. (c) Paddon-Row, M. N. *Acc. Chem. Res.* **1994**, *27*, 18.
(3) (a) Zeng, Y.; Zimmt, M. B. *J. Phys. Chem.* **1992**, *96*, 8395. (b) Oliver, A. M.; Paddon-Row, M. N.; Kroon, J.; Verhoeven, J. W. *Chem. Phys. Lett.* **1992**, *191*, 371.
(4) (a) Closs, G. L.; Miller, J. R. *Science* **1988**, *240*, 440. (b) Guldi, D. M.; Luo, C.; Prato, M.; Troisi, A.; Zerbetto, F.; Scheloske, M.; Dietel, E.; Bauer, W.; Hirsch, A. *J. Am. Chem. Soc.* **2001**, *123*, 9166.
(5) Napper, A. M.; Head, N. J.; Oliver, A. M.; Shephard, M. J.; Paddon-Row, M. N.; Read, I.; Waldeck, D. H. *J. Am. Chem. Soc.* **2002**, *124*, 10171.

Scheme 1

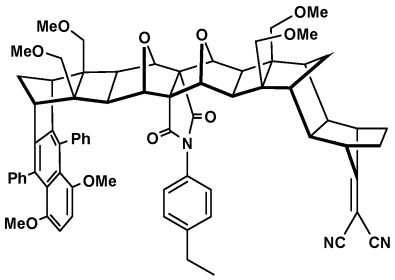

1DBA

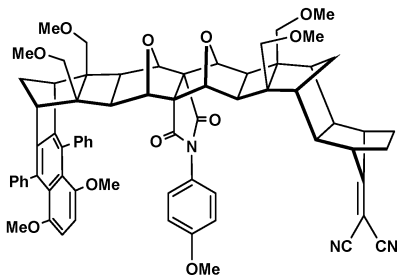

2DBA

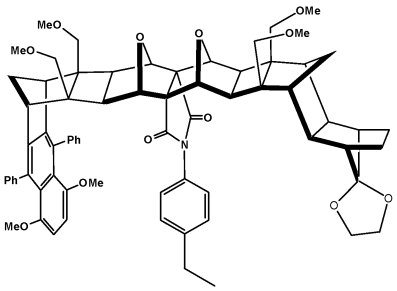

1DB

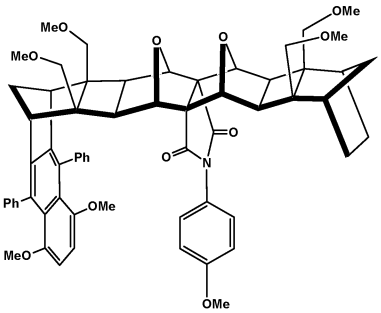

2DB

substituted phenyl groups have similar electronic couplings.[6]

The current work investigates the photoinduced electron-transfer kinetics and charge-transfer emission spectra of the U-shaped DBA molecule **2DBA**, bearing a *p*-methoxyphenyl pendant group in different aromatic solvents, and compares it with the previously studied molecule **1DBA**, having an ethyl-substituted phenyl group (Scheme 1). This allows us to explore how the electronic nature of the pendant group affects the electronic coupling. The molecules **1DBA** and **2DBA** have the same 1,4 diphenyl-5,8-dimethoxynaphthalene (**DPMN**) donor unit and 1,1-dicyanovinyl (**DCV**) acceptor unit connected through a highly curved bridge unit which holds the donor and the acceptor moieties at a particular distance and orientation. A pendant group is covalently attached to the bridge and occupies the space between the donor and the acceptor. It has been shown that the electron tunnels from the donor to the acceptor unit through the "*line-of-sight*" noncovalent linkage between the donor and the acceptor.[7] It has been established that the electron-transfer mechanism in **1DBA** is nonadiabatic at high temperature and in solvents with rapid solvation responses. In this mechanistic limit, the electron tunneling probability is proportional to the square of the electronic coupling, $|V|^2$.

The schematic energy diagram in Figure 1 shows an effective one-dimensional nuclear reaction coordinate. Two possible electron-transfer regimes are distinguished by the strength of the electronic coupling $|V|$, the interaction between the reactant and the product states at the curve crossing. When the electronic coupling is weak $|V| \ll k_B T$, the reaction is nonadiabatic (dashed curve going through the dashed line at the curve crossing point in Figure 1), and the rate constant is proportional to $|V|^2$. In this regime, the system may move through the curve-crossing region many times before the electronic state changes. The second regime is adiabatic electron transfer, where $|V| \gg k_B T$ (dashed curves going through the solid line at the curve-crossing point in Figure 1). In this limit, the electronic state change evolves as the nuclear motion proceeds; i.e., the strong coupling mixes the donor and acceptor states, and the reaction proceeds along a single electronic state. A third regime is friction-controlled electron transfer, in which the electronic coupling is weak but the polarization response of the solvent is slow enough that nearly every passage through the crossing region results in a change of electronic state.

For the U-shaped molecules **1DBA**, the electronic coupling between the donor and acceptor moieties is weak enough that the electron transfer lies in the nonadiabatic limit. The semiclassical model for electron transfer in or near the nonadiabatic limit begins with a Fermi's Golden Rule expression for the transition rate; namely

$$k_{ET} = (2\pi/\hbar)|V|^2 \,\mathrm{FCWDS} \qquad (1)$$

where $\hbar$ is Planck's constant divided by 2π, $|V|$ is the electronic coupling matrix element, and FCWDS is the Franck−Condon weighted density of states. The FCWDS term accounts for the probability that the system achieves a nuclear configuration in which the electronic state can change. The square of the coupling, $|V|^2$ is proportional to the probability of changing from the reactant state to the product state.

Previous work successfully applied the Golden Rule rate constant expression to **1DBA** with a single effective quantum

(6) Liu, M.; Chakrabarti, S.; Waldeck, D. H.; Oliver, A. M.; Paddon-Row, M. N. *Chem. Phys.* **2006**, *324*, 72.
(7) Napper, A. M.; Read, I.; Waldeck, D. H.; Head, N. J.; Oliver, A. M.; Paddon-Row, M. N. *J. Am. Chem. Soc.* **2000**, *122*, 5220.

mode,

$$k_{ET} = \frac{4\pi^2}{h}|V|^2 \frac{1}{\sqrt{4\lambda_o \pi k_B T}} \sum_{n=0}^{\infty} \exp(-S)\left(\frac{S^n}{n!}\right) \exp\left[-\frac{(\Delta_r G + \lambda_o + nh\nu)^2}{4\lambda_o k_B T}\right] \quad (2)$$

where λ_o is the solvent reorganization energy; $\Delta_r G$ is the reaction free energy; $S = \lambda_v/h\nu$ and λ_v is the internal reorganization energy. The $h\nu$ term is the average energy spacing of a single effective quantized mode frequency in the electron-transfer reaction and is a characteristic of the donor and acceptor groups. The sum is performed over the vibrational states of the effective quantum mode.

The quantities $h\nu$ and λ_v are determined primarily by the donor and acceptor groups and are insensitive to their separation distance. A previous analysis of charge-transfer absorption and emission spectra in hexane solution for a DBA compound with the same donor and acceptor groups provides a reasonable estimate of these two parameters.[8] This analysis uses a value of 1600 cm^{-1} for the single effective quantized mode and 0.63 eV for the internal reorganization energy λ_v. This effective frequency is comparable to typical carbon−carbon stretching frequencies in aromatic ring systems, such as the naphthalene. A detailed analysis of how this choice affects the $|V|$ extracted from the data and the impact of introducing a lower-frequency mode, such as 1088 cm^{-1} for out-of-plane bending of the dicyanovinyl group, on the absolute magnitude of $|V|$ has been reported.[9]

In previous work, the three remaining parameters contained in the semiclassical rate expression (eq 2), namely λ_o, $|V|$, and $\Delta_r G$, were determined by measuring the temperature dependence of k_{ET} and using Matyushov's molecular solvation model.[10,11] The reaction Gibbs energies $\Delta_r G$ of **1DBA** in toluene, mesitylene, and *p*-xylene were experimentally measured from an analysis of the equilibrium between the locally excited state and the charge-separated state, and they were used to calibrate the molecular solvation model.[6,12] The solvation model, parametrized in this way, was also used to fit the photoinduced electron-transfer reaction rate constant in **1DBA**. This rate constant model is used to analyze the photoinduced electron transfer behavior of **2DBA** and **1DBA** in different aromatic solvents and obtain the electronic coupling for charge separation ($|V_{CS}|$) in these two compounds. In marked contrast to **1DBA**, compound **2DBA** displayed charge-transfer emission bands in nonpolar solvents, thereby providing the opportunity to determine the Gibbs energy, the reorganization energy, and the electronic coupling for charge recombination process ($|V_{CR}|$)

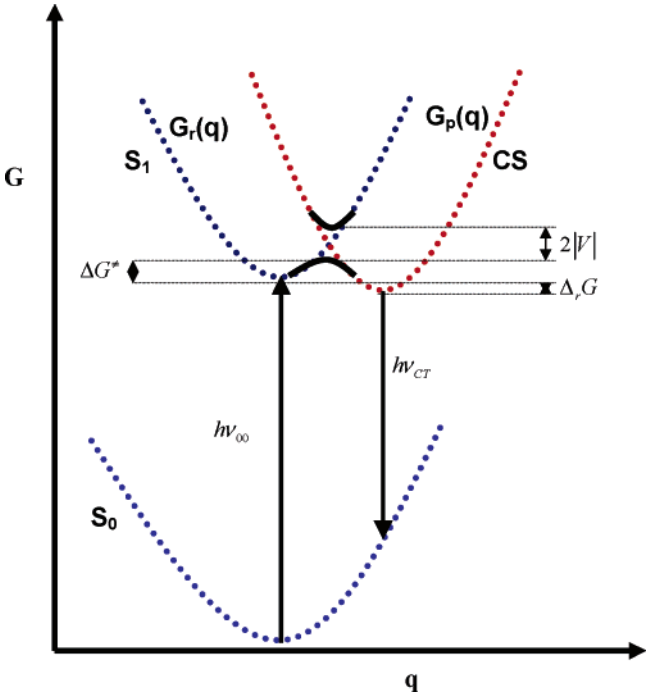

Figure 1. Gibbs energy G versus the nuclear coordinate q for the adiabatic (proceeding along the solid line at the curve crossing point)-strong coupling and non-adiabatic (proceeding along the diabatic dashed line at the curve cross point)-weak coupling mechanisms. S_1 is the locally exited state, CS is the charge-separated state, and S_0 is the ground state.

in **2DBA**. The results obtained from the charge-transfer emission band analysis are compared to the results obtained from the temperature-dependent rate analysis and molecular solvation model analysis. These analyses show that the magnitude of the electronic coupling for charge separation, $|V_{CS}|$, for **2DBA** is greater than that for **1DBA**. We also found that the strength of the electronic coupling for charge recombination, $|V_{CR}|$, from the charge-separated state to the ground state in **2DBA** is greater than that for charge separation, $|V_{CS}|$, for the same molecule. This finding may be attributed to differences in molecular geometry in the charge-separated and ground state of these molecules.

Experimental Section

Synthesis. The synthesis of the U-shaped supermolecules **1DBA** and **2DBA** followed established methodology[13] and full details are provided in the Supporting Information.

Time-Resolved Fluorescence Studies. Each sample was dissolved in the solvent at a concentration that gave a peak optical density of less than 0.2 at 330 nm. The solvent acetonitrile (99.9% HPLC) was purchased from Burdick & Jackson and used without further purification. The solvents toluene, mesitylene, and *p*-xylene were fractionally distilled two times using a vigreux column under vacuum after being purchased from Aldrich. The purified fraction was used immediately in all the experiments. The nonpolar solvent MCH was purchased from Aldrich and used without further purification. Each solution was freeze−pump−thawed a minimum of five cycles.

Each sample was excited at 330 nm by the frequency-doubled cavity-dumped output of a Coherent CR599-01 dye laser, using DCM (4-dicyanomethylene-2-methyl-6-*p*-dimethylamino-styryl-4H-pyran) dye, which was pumped by a mode-locked Vanguard 2000-HM532 Nd:YAG laser purchased from Spectra-Physics. The dye laser pulse train

(8) (a) Oevering, H.; Verhoeven, J. W.; Paddon-Row, M. N.; Warman, J. M. *Tetrahedron* **1989**, *45*, 4751. (b) Oevering, M. N.; Paddon-Row, M. N.; Heppener, H.; Oliver, A. M.; Cotsaris, E.; Verhoeven, J. H.; Hush, N. S. *J. Am. Chem. Soc.* **1987**, *109*, 3258.
(9) Kumar, K.; Kurnikov, I. V.; Beratan, D. N.; Waldeck, D. H.; Zimmt, M. B. *J. Phys. Chem. A* **1998**, *102*, 5529.
(10) Read, I.; Napper, A. M.; Zimmt, M. B.; Waldeck, D. H. *J. Phys. Chem. A* **2000**, *104*, 9385.
(11) Matyushov, D. V.; Voth, G. A. *J. Chem. Phys.* **1999**, *111*, 3630.
(12) (a) Paddon-Row, M. N.; Oliver, A. M.; Warman, J. M.; Smit, K. J.; de Hass, M.P.; Oevering, H.; Verhoeven, J. W. *J. Phys. Chem.* **1988**, *92*, 6958. (b) Warman, J. M.; Smit, K. J.; de Hass, M. P.; Jonker, S. A.; Paddon-Row, M. N.; Oliver, A. M.; Kroon, J.; Oevering, H.; Verhoeven, J. W. *J. Phys. Chem.* **1991**, *95*, 1979.
(13) Head, N. J.; Oliver, A. M.; Look, K.; Lokan. N. R.; Jones, G. A.; Paddon-Row, M. N. *Angew. Chem., Int. Ed.* **1999**, 38, 3219.

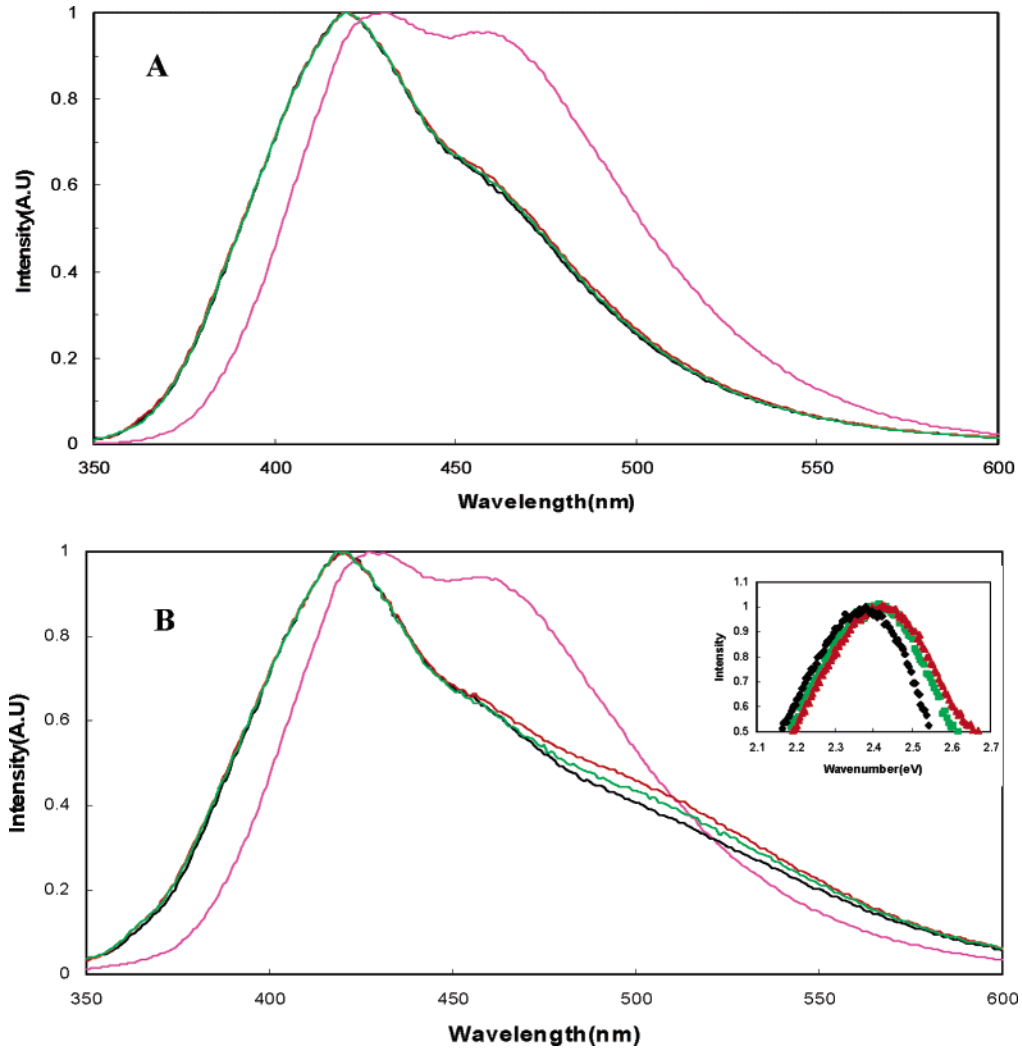

Figure 2. Steady-state emission spectra are shown for **2DBA** (panel B) and **1DBA** (panel A) in acetonitrile (pink), toluene (black), mesitylene (red) and *p*-xylene (green). The inset of panel B shows the difference spectra of **2DBA** and **2DB**.

had a repetition rate of 300 kHz. Pulse energies were kept below 1 nJ, and the count rates were kept below 3 kHz to prevent pile up effects. All fluorescence measurements were made at the magic angle, and data were collected until a standard maximum count of 10,000 was observed at the peak channel.

The steady-state and time-resolved fluorescence kinetics for **1DBA** and **2DBA** and their donor-only analogues (compound **1DB** and **2DB**) were carried out in different solvents as a function of temperature (OD $\approx$ 0.10). The temperature ranged from 273 K to a high of 346 K. The experimental temperature was controlled by an ENDOCAL RTE-4 chiller, and the temperature was measured using a Type-K thermocouple (Fisher-Scientific), accurate to within 0.1 °C.

The instrument response function was measured using a sample of colloidal $BaSO_4$. The fluorescence decay curve was fit by a convolution and compare method using IBH-DAS6 analysis software. Independent experiments on individual donor only molecules at the measured temperatures, always a single-exponential fluorescence decay, was used to determine the intrinsic fluorescence decay rate of the locally excited state. The DBA molecules, **1DBA** and **2DBA**, have a small amount of donor-only impurity. The measurement of the donor-only molecule's fluorescence decay characteristic for each solvent and temperature allowed their contribution to be subtracted from the decay law of the DBA molecules. The decay law of **1DBA** in acetonitrile was a single exponential function, but in the weakly polar and nonpolar solvents toluene, mesitylene, and *p*-xylene it was a double exponential function. The decay law for **2DBA** was single exponential in acetonitrile, and was nearly single exponential in the weakly polar and nonpolar solvents; i.e. the fit to a double exponential was superior, but the dominant component exceeded 99% in all cases.

Fitting of the charge-transfer emission spectra and rate constant to the semiclassical equation (eq 2) was performed using Microsoft Excel 2003. In fits to a molecular solvation model the electronic coupling was treated as an adjustable parameter for each solute molecule, and the reorganization energy at 295 K was treated as an adjustable parameter for each solvent type. The internal reorganization parameters were obtained from the charge-transfer spectra of the similar compound[6] and were kept fixed since the solute has the same donor and acceptor group. The reaction Gibbs energy for **1DBA** was obtained from the experimental data except in the polar solvent acetonitrile. The experimental $\Delta_r G$ data were used to parametrize the molecular solvation model and predict the $\Delta_r G$ for **1DBA** in acetonitrile and the $\Delta_r G$ for **2DBA**. The charge-transfer emission spectral analysis of **2DBA** was also used to determine the Gibbs energy, the electronic coupling, and the reorganization energy in different aromatic solvents.

Results

A. Emission Spectroscopy. Figure 2 shows the steady-state emission spectra of **1DBA** and **2DBA** recorded in the polar solvent acetonitrile, the weakly polar solvent toluene, and the

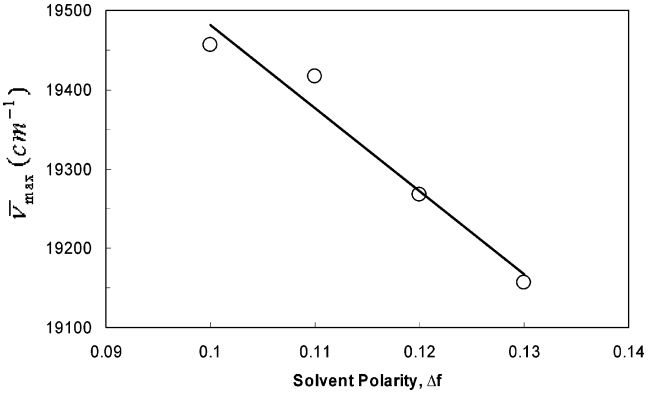

Figure 3. Lippert−Mataga plot is shown for the charge-transfer emission band of compound **2DBA** in different solvents.

nonpolar solvents mesitylene and *p*-xylene. The spectral features of the DBA molecules, **1DBA** and **2DBA**, are dominated by the 1,4-dimethoxy-5,8-diphenylnaphthalene donor unit with two dominant transition bands in the UV region assigned to the $^1A \rightarrow {}^1L_b$, and the $^1A \rightarrow {}^1L_a$ transitions. [6] For **1DBA** the steady-state emission spectra in weakly polar and nonpolar solvents are very similar (panel A), whereas the polar solvent acetonitrile changes the relative intensity of the two peaks and shifts them to the red. A similar emission spectrum was observed for **2DBA** in acetonitrile.

For **2DBA** the steady-state spectra in weakly polar and nonpolar solvents display three peaks (panel B) rather than the two peaks observed for **1DBA** (panel A). The locally excited (LE) emission bands for **2DBA** have the same position as those for **1DBA** in all these solvents, but a new spectral band is evident to the red. This weak red band shifts further to the red with increasing solvent polarity (see the inset of panel B, which shows the difference of the spectra for **2DBA** and **2DB** in the different solvents). This emission band is not observed for **2DBA** in the most polar solvent acetonitrile. These properties indicate that this emission is a charge-transfer ($CS \rightarrow S_0$) emission band.[12,14] Difference spectra of **2DBA** and **2DB** in different solvents are shown in the inset of Figure 2 (also see Figure 3) and were used to calculate values of $\bar{\nu}_{max}$. The solvent parameters and the resulting $\bar{\nu}_{max}$ values are listed in Table 1.We have analyzed the solvent dependence of the charge-transfer fluorescence maximum of compound **2DBA** in terms of the well-known Lippert−Mataga relation (eq 3).[15,16] The frequency of the charge-transfer emission band's maximum intensity is given by

$$\bar{\nu}_{max} = \left[\frac{-2\Delta\vec{\mu}^2}{hca^3}\right]\Delta f + \bar{\nu}^0_{max} \qquad (3)$$

where $\Delta f = [(\epsilon - 1)/(2\epsilon + 1)] - [(n^2 - 1)/(4n^2 + 2)]$, $\bar{\nu}_{max}$ is in cm^{-1}; $\bar{\nu}^0_{max}$ is the emission maximum for $\Delta f = 0$, a is the effective radius of a spherical cavity that the donor−acceptor molecule occupies in the solvent, $\Delta\vec{\mu} = |\vec{\mu}_{CS} - \vec{\mu}_{S_0}|$ is the difference in dipole moments of the charge-separated state and the ground state, h is Planck's constant, c is the velocity of light in vacuum, ϵ is the solvent dielectric constant, and n is the refractive index of the solvent. This result also incorporates the polarizability of the solute, which was taken equal to $1/3a^3$. The solvent parameter, Δf, depends on the static dielectric constant (ϵ_s) and refractive index (n) of the solvent, and it increases with increasing solvent polarity (see Table 1 and also Figure 3). The Δf parameter quantifies the solvent's ability to produce a macroscopic polarization in response to the newly formed charge distribution of the charge-separated state. Figure 3 shows a Lippert−Mataga plot for **2DBA** in the four solvents, where $\bar{\nu}_{max}$ of the charge-transfer emission band is plotted as a function of Δf. The plot clearly shows that $\bar{\nu}_{max}$ decreases as a function of increasing polarity, or Δf. A reasonable linear fit to the data provides a slope of -10500 cm^{-1}. To estimate $\Delta\vec{\mu}$ from this slope and eq 3, a cavity radius, a, of 7.66 Å was used. This value was chosen because previous work found it as a best fit to the $\Delta_r G$ data of **1DBA** to the molecular solvation model. Solving eq 3 for $\Delta\vec{\mu}$ gives a value of 22 D for the difference between the charge-separated state and the ground-state dipole moments. Using 5.75 D for the ground-state dipole moment[5] and assuming that the dipoles are collinear, the dipole moment of the charge-separated state is ∼28 D, which is close to the dipole moment of the charge-separated state used in the molecular solvation model analysis. This value is also in good agreement with the HF/3-21G calculated value of 28.6 D for a simulacrum of the charge-separated state of **1DBA** (the dipole moments of the charge-separated states of **1DBA** and **2DBA** should be similar).

Table 1. Charge-Transfer Emission Maxima ($\bar{\nu}_{max}$) of **2DBA** in Different Solvents at 295 K and Solvent Parameters, n, ϵ_s (295 K) and Δf for Each Solvent

solvent	n [a]	ϵ_s [a]	Δf	$\bar{\nu}_{max}$ (cm^{-1})
toluene	1.494	2.378	0.13	19157
mesitylene	1.496	2.271	0.12	19267
p-xylene	1.493	2.265	0.11	19417
MCH[b]	1.423	2.000	0.10	19457

[a] Zimmt, M. B; Waldeck, D. H. *J. Phys. Chem. A* **2003**, *107*, 3580. [b] MCH: methylcyclohexane.

Assuming that a unit charge is transferred, r_{dip} is equal to 5.8 Å for $|\mu_{CS}|$ of 28 D (i.e., the charge-transfer distance, r_{dip} can be estimated from the relation $r_{dip} = |\mu_{CS}|/e$),. This value is smaller than the UHF/3-21G calculated center-to-center distance of 8.7 Å between the **DPMN** donor and the **DCV** acceptor groups in the charge-separated state geometry of a cognate of **2DBA** (vide infra). Although the reason for this difference remains unclear, it may reflect the fact that the negative and positive charges are delocalized over the respective **DCV** and **DPMN** groups (as predicted by UHF/3-21G calculations). Consequently, calculation of r_{dip} assuming a point-charge model may not be appropriate. (The closest **DCV**−DPMN distance obtained from UHF/3-21G calculation in the charge-separated state of the aforementioned cognate is 6.8 Å, between a **DCV** nitrogen and a **DPMN** CH ring carbon atom.)

B. Analysis of Charge-Transfer Emission Spectra of 2DBA To Obtain $\Delta_r G$ and λ_o. The charge recombination driving force

(14) Wasielewski, M. R.; Minsek, D. W.; Niemczyk, M. P.; Svec, W. A.; Yang, N. C. *J. Am. Chem. Soc.* **1990**, *112*, 2823.
(15) Morais, J.; Huang, R. R.; Grabowski, J. J.; Zimmt, M. B. *J. Phys. Chem.* **1993**, *97*, 13138.
(16) (a) Mataga, N.; Kaifu, Y.; Koizumi, M. *Bull. Chem. Soc. Jpn.* **1955**, *28*, 690. (b) Mataga, N.; Kaifu, Y.; Koizumi, M. *Bull. Chem. Soc. Jpn.* **1955**, *29*, 465.

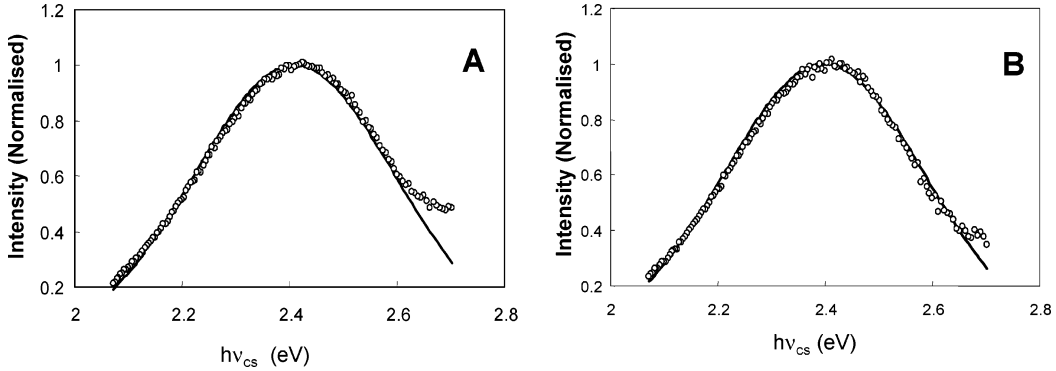

Figure 4. The figure shows experimental (○) and calculated (solid lines) charge-transfer emission spectra of **2DBA** in mesitylene (panel A) and in *p*-xylene (panel B). These spectra were calculated using $\lambda_v = 0.63$ eV, $\bar{\nu} = 1600$ cm^{-1}, $\lambda_o = 0.68$ eV (for mesitylene and *p*-xylene) and $\Delta_r G(\mathrm{CS} \rightarrow \mathrm{S_0}) = -3.288$ eV (mesitylene) and -3.277 eV (*p*-xylene).

Table 2. $\Delta_r G$ and λ_o; Determined from the Charge-Transfer Emission Spectra, Using $E_{00} = 3.40$ eV[a,b]

solvent	$\hbar\nu_{max}$ (eV)	ϵ	$\Delta G(\mathrm{CS} \rightarrow \mathrm{S_0})$ (eV)	λ_o (eV)
toluene	2.38	2.37	-3.26 ± 0.04	0.69 ± 0.02
mesitylene	2.39	2.27	-3.29 ± 0.01	0.68 ± 0.01
p-xylene	2.41	2.27	-3.28 ± 0.02	0.68 ± 0.01

[a] The E_{00} was obtained from the mirror point between absorption and emission spectra in mesitylene for compound **2DBA**. [b] The uncertainty in the parameter values and their correlation with each other are discussed in the Supporting Information.

Table 3. $\Delta_r G(\mathrm{LE} \rightarrow \mathrm{CS})$ values for **1DBA** and **2DBA** in Different Solvents

solvent	cmpd	$\Delta_r G$ (model) (eV)	$\Delta_r G$ (expt) (eV)
toluene	**1DBA**	-0.12	-0.12[a]
mesitylene	**1DBA**	-0.09	-0.08[a]
p-xylene	**1DBA**	-0.09	-0.09[a]
acetonitrile	**1DBA**	-0.55	
toluene	**2DBA**	-0.11	-0.14[b]
mesitylene	**2DBA**	-0.08	-0.11[b]
p-xylene	**2DBA**	-0.06	-0.12[b]
acetonitrile	**2DBA**	-0.54	

[a] Obtained from kinetic analysis and taken from ref 6. Reported here for sake of comparison. [b] Obtained from charge-transfer emission spectra fitting.

for **2DBA** was estimated by simulation of the charge-transfer emission line shape using the relation given by Marcus,[17] i.e.

$$I_{\mathrm{emission}}(\nu_{\mathrm{CS}}) = \sum_j \frac{e^{-S} S^j}{j!} \cdot \exp\left[-\frac{(jh\nu + \Delta G_{\mathrm{rec}} + \lambda_o + h\nu_{\mathrm{CS}})^2}{4\lambda_o kT} \right] \quad (4)$$

Figure 4 compares the experimental difference spectra to simulated spectra predicted by eq 4 in mesitylene (panel A) and *p*-xylene (panel B) respectively. Such fits provide estimates of $\Delta_r G(\mathrm{CS} \rightarrow \mathrm{S_0})$ and other electron-transfer parameters included in the semiclassical model: λ_o, λ_v, $h\nu$, and $\Delta_r G(\mathrm{CS} \rightarrow \mathrm{S_0})$. The Gibbs energy $\Delta_r G(\mathrm{LE} \rightarrow \mathrm{CS})$ can be obtained from $\Delta_r G(\mathrm{LE} \rightarrow \mathrm{CS}) = -\Delta_r G(\mathrm{CS} \rightarrow \mathrm{S_0}) - E_{00}$, where E_{00} is the excited-state energy of the donor unit. Because different combinations of the four parameters can accurately reproduce the experimental line shapes, the fitting parameters were constrained by using a constant value of 0.63 eV for the λ_v parameter and a value of $\bar{\nu} \approx 1600$ cm^{-1}; these values were used previously for similar molecules and were chosen for consistency with earlier work. Only λ_o and $\Delta_r G(\mathrm{CS} \rightarrow \mathrm{S_0})$ were adjusted in different solvents to optimize the fit. Table 2 lists the different values of $\Delta_r G(\mathrm{CS} \rightarrow \mathrm{S_0})$ and λ_o obtained from the charge-transfer spectral fitting for different solvents. The line-shape derived estimates of λ_o increases with increasing solvent dielectric constant.

In previous work $\Delta_r G(\mathrm{LE} \rightarrow \mathrm{CS})$ for **1DBA** was determined directly from the kinetic data by fitting the molecular solvation model to the experimental data for toluene, mesitylene and *p*-xylene and that model was calibrated to predict the free energy for the polar solvent acetonitrile.[6] In that analysis the radius of the solute was optimized and found to be 7.66 Å; the ground-state dipole moment was 5.75 D; and the excited-state dipole moment was 28.64 D. The same analysis was carried out to determine the $\Delta_r G(\mathrm{LE} \rightarrow \mathrm{CS})$ for **2DBA**. Because the fluorescence lifetime of **2DBA** was nearly single exponential (~99% or greater) at all the temperatures and in all the solvents, the reaction Gibbs energy could not be experimentally determined for **2DBA** using the kinetic rate data. This indicates that the Gibbs energy for **2DBA** is more negative than -0.13 eV and it cannot be determined directly from the experiment. This observation implies that $\Delta_r G$ for **2DBA** is more negative than that for **1DBA.** The charge-transfer fit parameters of **2DBA** in different solvents were used to determine the $\Delta_r G(\mathrm{LE} \rightarrow \mathrm{CS})$ for **2DBA.** Table 3 compares the $\Delta_r G$ of **1 DBA** and **2DBA.** The Gibbs energy becomes more negative as the solvent becomes more polar, progressing from mesitylene and *p*-xylene, which have the least negative $\Delta_r G(\mathrm{LE} \rightarrow \mathrm{CS})$, to toluene which is more negative, and finally to acetonitrile which is the most negative. Table 3 also reveals a reasonable agreement between the Gibbs energy for **2DBA** obtained from the charge-transfer emission spectral fitting and that predicted from the molecular solvation model.

C. Kinetic Analysis. With the reaction free energy and the internal reorganization energy parameters from the previous studies, it is possible to fit the temperature-dependent rate constant data and extract the electronic coupling $|V_{\mathrm{CS}}|$ and the solvent reorganization energy λ_o for the charge separation process. $|V_{\mathrm{CS}}|$ is treated as a temperature-independent quantity, whereas the solvent reorganization energy has a temperature dependence because the solvation is temperature dependent. The temperature dependence of the solvent reorganization energy

(17) (a) Marcus, R. A. *J. Phys. Chem.* **1989**, *93*, 3078. (b) Cortes, J.; Heitele, H.; Jortner, J. *J. Phys. Chem.* **1994**, *98*, 2527.

Table 4. Best Fit of Electronic Coupling and Reorganization Energy (from the Kinetic Fit and from Charge-Transfer Emission Spectra) for **1DBA** and **2DBA**

solvent	$\|V_{CS}\|$ (cm^{-1})[a]	$\|V_{CR}\|$ (cm^{-1})[b]	λ_o (eV)[c]	λ_o (eV)[d]
		1DBA		
toluene	147		0.70	
mesitylene	147		0.66	
p-xylene	147		0.67	
acetonitrile	147		1.50	
		2DBA		
toluene	274	467	0.79	0.69
mesitylene	274	453	0.75	0.68
p-xylene	274	512	0.72	0.68
acetonitrile	274		1.63	

[a] Coupling obtained from the best fit to the rate data. The values for **1DBA** were taken from ref 6 and are shown here for comparison. [b] Coupling obtained form the charge-transfer emission spectral analysis using the distance 5.8 Å. [c] Reorganization energy obtained from best fit rate data. [d] Reorganization energy obtained from the charge-transfer emission spectra fit.

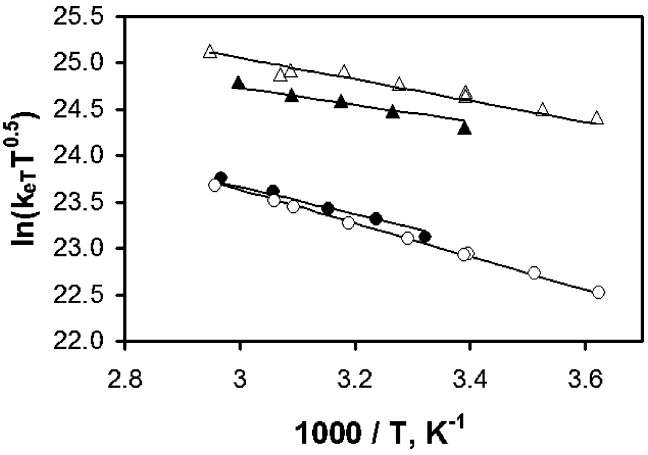

Figure 5. Experimental rate constant data are plotted versus 1/T, for **1DBA** in mesitylene (▲) and acetonitrile (●), and for **2DBA** in mesitylene (△) and in acetonitrile (○). The line represents the best fits to semiclassical equation.

was predicted from the molecular solvation model and the best fit was used to extract the solvent reorganization energy at 295 K, as described previously. The fit of the temperature-dependent rate constant data was used to determine the electronic coupling $|V_{CS}|$ and λ_o (295 K), listed in Table 4. Figure 5 shows fits of the experimental rate constant to the model for compound **1DBA** and **2DBA** in mesitylene and acetonitrile. The rate data in toluene and *p*-xylene behave similarly. The reverse order of the electron-transfer rate for **1DBA** and **2DBA** in mesitylene and acetonitrile can be explained by their different reorganization energy value. [The difference of reorganization energy between **1DBA** and **2DBA** is 0.09 eV in mesitylene, but in acetonitrile the difference is 0.13 eV. This higher difference of λ_o is responsible for reversal of the order.[18]]

Table 4 lists the solvent reorganization energies, λ_o, at 295 K and electronic couplings $|V_{CS}|$ that are obtained for the four solvents by fitting to the temperature dependent rate constant expression obtained from semiclassical model. The above findings, from the temperature dependent rate data analysis, show that the electronic coupling for charge separation in **2DBA** is stronger than that in **1DBA** by a factor of 1.9.

D. Calculation of the Electronic Coupling for Charge Recombination in 2DBA from CT Emission Spectra. Experimental evidence for a relatively close and solvent independent donor−acceptor distance in the charge-separated state was obtained from the radiative rate constant (k_r) for the charge-transfer fluorescence, which can be calculated from the fluorescence lifetime (τ) and quantum yield of the charge-transfer fluorescence (Φ) via $k_r = \Phi/\tau$. It has been shown that the radiative rate constant (in s^{-1}) can be expressed by eq 5.[19]

$$k_r = (0.714 \times 10^{-5}) n^3 R^2 |V_{CR}|^2 \bar{\nu}_{max} \qquad (5)$$

In eq 5, R is the interchromophore distance in Å, n is the refractive index, and $|V_{CR}|$ is the electronic coupling matrix element in cm^{-1}. Using the value of 5.8 Å for R, obtained from the Lippert−Mataga plot, one finds the electronic coupling values tabulated in Table 4. The electronic coupling for **2DBA**, $|V_{CR}|$ is approximately 500 cm^{-1}.

Table 4 shows that for **2DBA** the λ_o (295 K) values obtained from fitting to the charge-transfer emission spectra is less than the value obtained from the kinetic rate data. To analyze the error in the kinetic rate data fit, we have used different $\Delta_r G$ (295 K) values ranging from 0.06 to 0.10 eV in the fit to see how λ_o (295 K) changes. This analysis shows that a range of λ_o values from 0.70 to 0.79 eV are connected with the kinetic rate data. See the Supporting Information for details.

E. Theoretical Calculations. A fully optimized gas-phase geometry of the ground state of **2DBA** was obtained at the B3LYP/6-31G(d) level and is depicted in Figure 6a and b. The complete geometry optimization was carried out using Gaussian 03.[20]

The optimized ground-state structure of **2DBA** is very similar to that computed for **1DBA** and various pendant-phenyl-substituted cognates.[5,6,21] The pendant methoxyphenyl ring is twisted 48° with respect to the plane of the imide ring, the closest distance between the **DPMN** and **DCV** chromophore units is 9.2 Å which is between a CH carbon atom of the former and an N atom of the latter, and the closest distances between the pendant group and the **DPMN** and **DCV** chromophore units are 3.8−3.9 Å (cf. 47°, 9.4 Å, and 3.8−3.9 Å, respectively for the compound having methylphenyl as pendant group).

Because of the large sizes of these U-shaped molecules, it was not feasible to compute the optimized geometry of the locally excited state of **2DBA**, which is relevant to the mechanism of photoinduced charge separation, using the CIS method. The strong similarities found between the ground-state geometries of **1DBA** and **2DBA** most likely holds for the locally excited states of these systems. Consequently, the greater magnitude of the electronic coupling for photoinduced charge separation in **2DBA**, compared to that in **1DBA**, is unlikely to be caused by structural differences in the two systems. Two important classes of virtual ionic states, namely $^+$DPMN−

(18) When the fitting was done in acetonitrile keeping the difference of reorganization energy between **1DBA** and **2DBA** 0.09 eV (same as mesitylene), the molecular solvation theory predicts higher values of k_{ET} for **2DBA** than for **1DBA** but leads to a bad fit between the experimental and theoretical prediction of **2DBA**.

(19) Koeberg, M.; deGroot, M.; Verhoeven, J. W.; Lokan, N. R.; Shephard, M. J.; Paddon-Row, M. N. *J. Phys. Chem. A* **2001**, *105*, 3417.

(20) Frisch, M. J.; et al. Gaussian, Inc.: Pittsburgh PA, 2003.

(21) Liu, M.; Waldeck, D. H.; Oliver, A.; Head, N. J.; Paddon-Row, M. N. *J. Am. Chem. Soc.* **2004**, *126*, 10778.

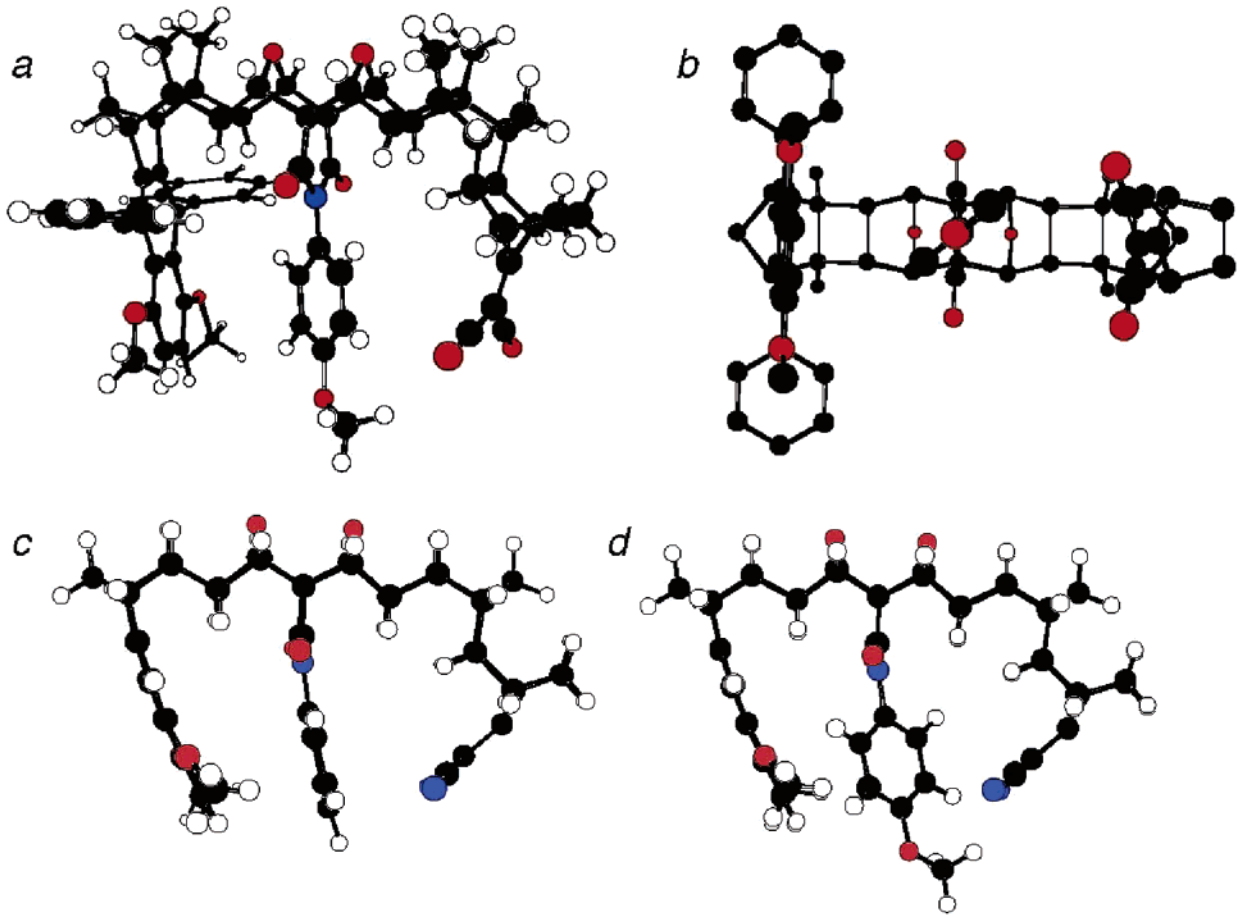

Figure 6. (a) B3LYP/6-31G(d) optimized ground-state geometry of **2DBA**. (b) As for (a) but looking along the major axis of the pendant *p*-methoxyphenyl group; the hydrogen atoms are omitted for clarity. (c) UHF/3-21G optimized geometry of the $^1A''$ charge-separated state of a simplified model for **1DBA**, referred to as **1DBA′** (i.e., **1DBA**, but with phenyl pendant group in place of *p*-ethylphenyl and with the dimethoxynaphthalene group in place of **DPMN**). The geometry was constrained to C_s symmetry. (d) Simulated geometry for the charge-separated state for **2DBA**, in which the bridge has the same geometry as that calculated for the charge-separated state of **1DBA′** but with the *p*-methoxyphenyl pendant twisted 48° out of the plane of the imide ring.

pendant$^-$ and $^+$pendant$-$DCV$^-$, contribute to the coupling for photoinduced electron transfer in these systems. However, for charge transfer from the locally excited state of the donor to the acceptor, the former ionic state is expected to be more important. Comparison with experimental data on monosubstituted benzenes suggests that the pendant groups' electron affinities (EA) (anisole EA = −1.09 eV and ethyl benzene EA = −1.17 eV[22]) are similar, but that **2DBA** should have a larger electronic coupling than **1DBA**. It may be that the second virtual ionic state $^+$pendant$-$DCV$^-$ contributes, when the pendant group has a low ionization potential (IP) value. The IPs for toluene and anisole are 8.83 and 8.39 eV, respectively.[23] Whether one coupling mechanism dominates over the other, could, in principle, be resolved by studying a U-shaped system in which an electron-withdrawing group is attached to the pendant aromatic ring at position 3 or 4. Unfortunately, all attempts to synthesize such a system have so far met with failure.

Earlier UHF/3-21G gas-phase calculations of charge-separated states revealed remarkable electrostatically driven changes in their geometries, compared to their ground-state structures.[5,19,24] Regarding the U-shaped systems discussed in this paper, we were successful only in optimizing, at the UHF/3-21G level, the geometry of the charge-separated state of a cognate of **1DBA**, termed as **1DBA′**, in which the pendant group was phenyl and the dimethoxynaphthalene group, **DMN**, was the donor moiety (in place of **DPMN**). Furthermore, the geometry of the charge-separated state of **1DBA′** was constrained to possess C_s symmetry;[25] within this constraint, the electronic state of this charge-separated state is $^1A''$, thereby preventing collapse of the wavefunction to the $^1A'$ ground state during the geometry optimization. [24,25] The resulting optimized gas-phase structure for the charge-separated state of **1DBA′** is shown in Figure 6c, a particularly noteworthy feature being the strong pyramidalization of the **DCV** anion radical toward the **DPMN** cation radical whose rings are slightly bent, in the direction of the **DCV** moiety. Due to the imposed C_s symmetry constraint, the phenyl pendant group is roughly parallel to the imide ring. Such a conformation, in which the phenyl ring eclipses the imide

(22) Jordan, K. D.; Burrow, P. D. *Acc. Chem. Res.* **1978**, *11*, 341.
(23) Toluene: Kimura, K. *Handbook of He(I) photoelectron spectra of fundamental organic molecules*; Japan Scientific Societies Press: Tokyo, 1981. Anisole: Kobayashi, T.; Nagakura, S. *Bull. Chem. Soc. Japan* **1974**, *47*, 2563.
(24) (a) Shephard, M. J.; Paddon-Row, M. N. *J. Phys. Chem. A* **1999**, *103*, 3347. (b) Shephard, M. J.; Paddon-Row, M. N. *J. Phys. Chem. A* **2000**, *104*, 11628.
(25) Fully optimized charge-separated state geometries, with no symmetry constraints, could be calculated using some sort of CI procedure, the simplest being CIS. However, preliminary attempts to optimize the charge-separated state of **1DBA′**, even using the relatively small 3-21G basis set, met with such huge computational overheads that they were aborted.

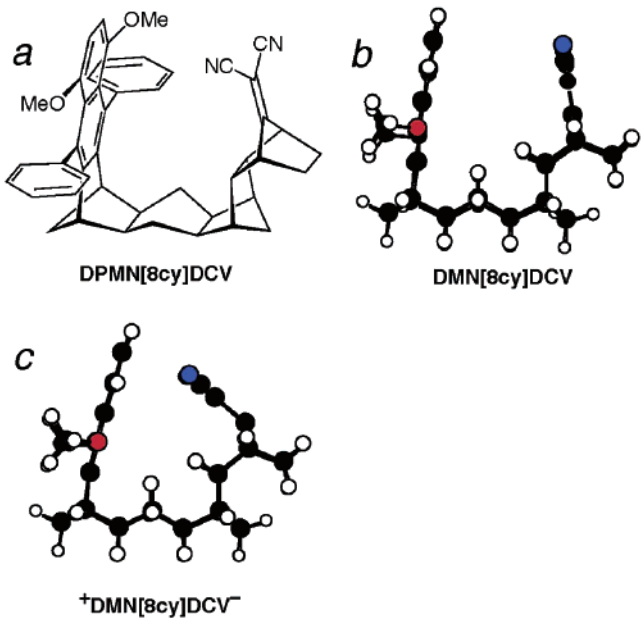

Figure 7. (a) Schematic of **DPMN[8cy]DCV**. (b) HF/3-21G optimized ground-state structure of the cognate **DMN[8cy]DCV**, bearing the dimethoxynaphthalene donor in place of **DPMN**, and (c) UHF/3-21G optimized geometry of the $^1A''$ charge-separated state of **DMN[8cy]DCV**, constrained to C_s symmetry.

carbonyl groups, should be unstable, as it is in the ground state, and the relaxed phenyl−imide conformation in the charge-separated state of **1DBA′** should resemble that computed for the ground-state structure, i.e., with the phenyl ring twisted 48° with respect to the imide plane as depicted by the simulated structure in Figure 6d.

The calculated UHF/3-21G dipole moment of **1DBA′** is 28.6 D[5] which is in good accord with the value of 28 D for **2DBA**, determined from the Lippert−Mataga plot. Also the distance between the centroids of the **DPMN** and **DCV** chromophore units in **1DBA′** was calculated to be 8.7 Å, although the closest contact between non-hydrogen atoms of the donor and acceptor groups is only 6.8 Å. The closest non-hydrogen atom contacts between the pendant group in the charge-separated state of **1DBA′** and the **DMN** and **DCV** chromophores are 3.6 and 3.2 Å, respectively, and these are even smaller in the more reasonable structure depicted in Figure 6d: 2.65 and 2.7 Å, respectively. The significantly smaller chromophore-pendant contacts of 2.7 Å in the simulated charge-separated state (Figure 6d), compared to 3.8 Å in the ground state of **1DBA** (Figure 6a) could well be responsible for the observed stronger electronic coupling of 453−512 cm^{-1} for charge recombination compared to charge separation, which is 274 cm^{-1} in **2DBA**.

Discussion

The electron-transfer rate constant from the locally excited-state of **DPMN** to **DCV** for **2DBA** is larger than that for **1DBA** in toluene, mesitylene, and *p*-xylene solvents. This increase arises from the greater magnitude of the electronic coupling in **2DBA**, as found from analysis of the temperature-dependent rate data. It is important to note that the electronic coupling obtained from the charge-transfer emission is the coupling between the charge-separated state and the ground state (the charge recombination pathway), whereas the kinetic rate data provide the coupling between the locally excited state and the charge-separated state. Whereas **1DBA** does not display charge-transfer fluorescence, **2DBA** does, presumably because the magnitude of $|V_{CR}|$ for **2DBA** is substantially larger than for **1DBA**. Although the charge-transfer emission for **2DBA** is also not observed in acetonitrile, it is likely because of the nonradiative charge recombination decay being rapid in this solvent. As the solvent polarity increases, the driving force for charge recombination decreases and, within the context of the Marcus "inverted region", the rate of the nonradiative recombination process increases and becomes the dominant pathway in acetonitrile, quenching the charge-transfer emission. The same effect was observed by Koeberg et al. in their study of the 8-bond U-shape system **DPMN[8cy]DCV** (Figure 7a), which exhibited charge-transfer fluorescence in weakly polar solvents but not in polar ones.[19]

It is illuminating to compare the strength of the electronic coupling for charge-transfer fluorescence of ∼500 cm^{-1} for **2DBA** with the value of 374 cm^{-1} (in benzene) for **DPMN-[8cy]DCV**.[19] Both systems possess similar U-shape configurations, but the latter lacks a pendant group. Even though the **DPMN** and **DCV** chromophores are connected by *twelve* bonds in **2DBA**, compared to only *eight* bonds in **DPMN[8cy]DCV** (see Figure 7a), the electronic coupling strength for charge-transfer fluorescence in the former molecule is larger than that for the latter. This observation is best understood if the charge recombination (and charge separation) in **2DBA** takes place by the through-pendant mechanism, rather than by a through-bridge (i.e., through-bond) mechanism. The charge recombination mechanism in **DPMN[8cy]DCV** is discussed below.

An even more convincing demonstration of the extraordinarily large strength of the electronic coupling element for charge-transfer fluorescence in **2DBA** is to compare its magnitude (∼500 cm^{-1}) with those for charge-transfer fluorescence in the series **DMN-*n*-DCV**, in which the donor and acceptor chromophores are connected to rigid norbornylogous bridges, *n* bonds in length, which possess the all-*trans* configuration.[8a] This all-*trans* configuration in **DMN-*n*-DCV** guarantees that electron transfer in these molecules takes place by the through-bond mechanism.[2c]

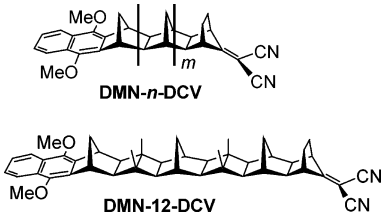

Extrapolating the experimental $|V_{CR}|$ values[8a] for the 4-, 6-, 8-, and 10-bond systems leads to a predicted $|V_{CR}|$ value of ∼6 cm^{-1} for the 12-bond system **DMN-12-DCV**. Because the 12-bond norbornylogous bridge in **2DBA** possesses *two* cisoid kinks, through-bridge-mediated electronic coupling in this molecule should be significantly *weaker* than that through the all-*trans* bridge in **DMN-12-DCV**.[2b,c] In fact $|V_{CR}|$ for **2DBA** is ∼90 times *stronger* than that estimated for **DMN-12-DCV**. Clearly, charge recombination from the charge-separated state of **2DBA** is not taking place by a through-bridge-mediated mechanism. These findings, together with the observation that the strength of the electronic coupling for photoinduced charge separation for **2DBA** is greater than that for **1DBA** leads to the

unequivocal conclusion that charge separation and charge recombination processes must be taking place via the pendant aromatic ring in both **2DBA** and **1DBA**.

There is strong evidence that charge recombination in **DPMN[8cy]DCV** takes place directly, through space, between the two chromophores, which is facilitated by the electrostatically enforced proximity of the two chromophores in the charge-separated state of this species (see Figure 7c). Thus, the distance between the two centroids in the charge-separated state of **DPMN[8cy]DCV**, based on a model system (Figure 7c), is only 4.4 Å,[19] which is sufficiently small to promote strong through-space interchromophore coupling in this species.[26] The distances between the pendant group and **DPMN** and **DCV** chromophores in the charge-separated state of **1DBA′** are between 3.4 and 2.7 Å, depending on the twist angle of the pendant phenyl ring (see previous section). These distances are significantly smaller than the aforementioned value computed for the charge-separated state of **DPMN[8cy]DCV**. Thus, the finding that the strength of the electronic coupling for charge-transfer fluorescence is substantially larger for **2DBA**, compared to that for **DPMN[8cy]DCV**, is understandable.

A fit of the rate constant data as a function of temperature to eq 2 was used to extract values for the solvent reorganization energy (see Table 4) for **1DBA** and **2DBA**. The solvent reorganization energy values of **2DBA** are higher than those for **1DBA** in all the solvents. The differences between their solvent reorganization energy values are highest for the most polar solvent acetonitrile and least for *p*-xylene. Since the pendant groups in **1DBA** and **2DBA** have comparable sizes, the difference is likely caused by differences in the polarities of the pendant groups in these molecules, the electronegative oxygen atom making the methoxyphenyl pendant group in **2DBA** more polar than ethylphenyl group in **1DBA**. The charge-transfer emission fit was also used to determine the solvent reorganization energy for charge recombination in **2DBA** (Table 4). The values obtained from charge-transfer emission spectra fitting is somewhat smaller than the values obtained from the kinetic rate data and correlates with more negative values of $\Delta_r G$ obtained from charge-transfer emission fit (Table 3).

The $\Delta_r G$ values for **1DBA** were obtained from the kinetic fit of the experimental data by the molecular solvation model whereas fitting to the charge-transfer emission was used to calculate $\Delta_r G$ values of **2DBA** experimentally in different solvents. The magnitude of $\Delta_r G$ is least negative in *p*-xylene and is most negative in the polar solvent acetonitrile. The $\Delta_r G$ for **2DBA** cannot be determined from a kinetic fit as $\Delta_r G$ is too negative (from charge-transfer emission fitting); however, the estimated free energy obtained from the molecular solvation model for **2DBA** is somewhat lower than the free energy of **1DBA**. This finding indicates that there is some error associated with the fitting. To estimate the error we have used the contour plot of reorganization energy values as a function of different free energy values in the fit in mesitylene (see the Supporting Information). The plot provides reasonable values for the reorganization energy ranging from 0.70 to 0.79 eV and $\Delta_r G$ values close to the values obtained from the charge-transfer emission fit.

Conclusion

The electron transfer in U-shaped molecules **1DBA** and **2DBA** containing two different pendant groups in the cleft between the donor and acceptor group was studied. **2DBA** shows charge-transfer emission in nonpolar and weakly polar solvents. The magnitudes of the electronic coupling for photoinduced charge separation in **1DBA** and **2DBA** were found to be 147 and 274 cm^{-1}, respectively. The origin of this difference lies in the electronic nature of the pendant aromatic group, since charge separation occurs by tunneling through the pendant group, rather than through the bridge. The charge-transfer fluorescence for **2DBA** in nonpolar solvents was used to determine the electronic coupling for charge recombination, $|V_{CR}|$, the magnitude of which is $\sim$500 cm^{-1}, much larger than that for charge separation. This difference can be explained by changes in the geometry of the molecule in the relevant states; because of electrostatic effects, the **DPMN** and **DCV** chromophores are about 1 Å closer to the pendant group in the CS state than in the locally excited state. Consequently the through-pendant-group electronic coupling is stronger in the CS state—which controls the charge-transfer fluorescence process—than in the locally excited state—which controls the CS process. The magnitude of $|V_{CR}|$ for **2DBA** is almost 2 orders of magnitude greater than that in **DMN-12-DCV**, having the same length bridge as for the former molecule, but lacking a pendant group. This result unequivocally demonstrates the operation of the through-pendant-group mechanism of electron transfer in the pendant-containing U-shaped systems of the type **1DBA** and **2DBA**. Our observation of the modulation of the strength of electronic coupling in the U-shaped system **2DBA**, brought about by electrostatically driven changes in molecular geometry, suggests an intriguing approach to the generation of long-lived charge-separated species: build a U-shaped system possessing a doubly positively charged acceptor, $D-B-A^{2+}$ (e.g., A^{2+} = viologen). Photoinduced electron transfer should generate $D^{+}-B-A^{+}$. Repulsive electrostatic interactions should drive the singly positively charged chromophores further apart, thereby weakening the electronic coupling for charge recombination. Such an effect has been observed and explained in terms of this mechanism.[27]

Acknowledgment. We acknowledge financial support from the Australian Research Council and the U.S. National Science Foundation (CHE-041545).

Supporting Information Available: Synthesis, characterization, and rate constant data in different solvents of **1DBA** and **2DBA** and complete reference 20. This material is available free of charge via the Internet at http://pubs.acs.org.

JA067266B

(26) Paddon-Row, M. N.; Jordan, K. D. Through-Bond and Through-Space Interactions in Unsaturated Hydrocarbons: Their Implications for Chemical Reactivity and Long-Range Electron Transfer. In *Modern Models of Bonding and Delocalization*; Liebman, J. F., Greenberg, A., Eds.; VCH Publishers: New York, 1988; Vol. 6, p 115.

(27) (a) Jolliffe, K. A.; Bell, T. D. M.; Ghiggino, K. P.; Langford, S. J.; Paddon-Row, M. N. *Angew. Chem., Int. Ed.* **1998**, *37*, 916. (b) Bell, T. D. M.; Jolliffe, K. A.; Ghiggino, K. P.; Oliver, A. M.; Shephard, M. J.; Langford, S. J.; Paddon-Row, M. N. *J. Am. Chem. Soc.* **2000**, *122*, 10661.